Radiology: Imaging Cancer

TECHNICAL DEVELOPMENT

Prospective Multireader Evaluation of Photon-counting CT for Multiple Myeloma Screening

Fides R. Schwartz, MD • Emily N. Vinson, MD • Charles E. Spritzer, MD • Roy Colglazier, MD • Ehsan Samei, PhD • Robert J. French, MD • Nicholas Said, MD • Leah Waldman, MD • Erin McCrum, MD

From the Department of Radiology, Duke University Health System, 2301 Erwin Rd, Box 3808, Durham, NC 27110. Received May 25, 2022; revision requested June 8; revision received August 31; accepted October 26. **Address correspondence to** F.R.S. (email: *fides.schwartz@duke.edu*).

E.S. supported by departmental funding from Siemens Healthineers.

Conflicts of interest are listed at the end of this article.

Radiology: Imaging Cancer 2022; 4(6):e220073 • https://doi.org/10.1148/rycan.220073 • Content codes: CT MK OI

Purpose: To determine whether photon-counting CT (PCCT) acquisition of whole-body CT images provides similar quantitative image quality and reader satisfaction for multiple myeloma screening at lower radiation doses than does standard energy-integrating detector (EID) CT.

Materials and Methods: Patients with monoclonal gammopathy of undetermined significance prospectively underwent clinical noncontrast whole-body CT with EID and same-day PCCT (August–December 2021). Five axial scan locations were evaluated by seven radiologists, with 11% (eight of 70) of images including osteolytic lesions. Images were shown in randomized order, and each reader rated the following: discernibility of the osseous cortex and osseous trabeculae, perceived image noise level, and diagnostic confidence. Presence of lytic osseous lesions was indicated. Contrast-to-noise ratio (CNR) and signal-to-noise ratio (SNR) were calculated. Comparisons were made using paired *t* tests and mixed linear effects models.

Results: Seven participants (four women) were included (mean age, 66 years ± 9 [SD]; body mass index, 30.1 kg/m^2 ± 5.2). Mean cortical definition, trabecular definition, image noise, and image quality scores were 83, 67, 75, and 78 versus 84, 66, 74, and 76 for EID and PCCT, respectively (P = .65, .11, .26, and .11, respectively). PCCT helped identify more lesions (79% [22 of 28]) than did EID (64% [18 of 28]). CNRs and SNRs were similar between modalities. PCCT had lower radiation doses than EID (volume CT dose index: EID, 11.37 ± 2.8 vs PCCT, 1.8 ± 0.6 [P = .06]; dose-length product: EID, 1654.1 ± 409.6 vs PCCT, 253.4 ± 89.6 [P = .05]).

Conclusion: This pilot investigation suggests that PCCT affords similar quantitative and qualitative scores as EID at significantly lower radiation doses.

Supplemental material is available for this article.

Multiple myeloma is a cancer of plasma cells originating in the bone marrow that can cause destructive bone lesions. Up to 70% of patients with multiple myeloma have osteolytic lesions at time of presentation, and whole-body CT is recommended by the European Myeloma Network and the European Society for Medical Oncology as the initial tool to help detect these lesions (1–3). Approximately 155 000 patients worldwide are newly diagnosed with multiple myeloma every year. Although there is currently an 82% median 5-year survival for patients with multiple myeloma, approximately 100 000 patients continue to die annually from the disease (4). While treatments are continually advancing, treatment efficacy highly depends on early-stage diagnosis, with whole-body CT as the imaging method of choice for the initial detection of osteolytic lesions (5,6). If osteolytic lesions are detected, both monoclonal gammopathy of undetermined significance and smoldering multiple myeloma are upstaged, altering treatment (3). Imaging is also used to monitor treatment response, with patients often undergoing multiple whole-body CT scans over the course of their illness (7). The standard radiation dose for a whole-body CT scan is 12 mGy (8), with up to 16 mGy delivered to the gonads and other radiation-sensitive organs (9).

Standard CT technology employs energy-integrating detectors (EID) that measure the total energy detected across multiple photons simultaneously (10). In contrast, photon-counting CT (PCCT) is a new technology that uses detectors that discriminate the energy of individual photons in the x-ray beam. PCCT has the capability to convert detected individual photons into electric signals (11). This offers multiple advantages over standard CT, including uniform photon weighting across multiple x-ray energies with improved image quality; small detector pixel design, which increases spatial resolution; energy thresholding, which eliminates electronic image noise; and energy binning, which permits the detection and quantification of multiple materials to enhance tissue characterization. The net result of PCCT is improved image quality and reproducibility (12,13).

The impact of this new-generation CT on the evaluation of multiple myeloma is not yet known. We hypothesize that PCCT can perform as well as EID in multiple myeloma screening, at a lower radiation dose. The purpose of this study is to determine whether PCCT acquisition of whole-body CT images provides similar quantitative image quality and reader satisfaction for multiple myeloma screening at lower radiation doses than does standard EID CT.

Abbreviations

CNR = contrast-to-noise ratio, EID = energy-integrating detector CT, PCCT = photon-counting CT, SNR = signal-to-noise ratio

Summary

Preliminary experience shows that photon-counting CT may provide similar quantitative image quality and reader assessment as standard energy-integrating detector CT, at a significantly reduced radiation dose, for screening of multiple myeloma.

Key Points

- In this head-to-head comparison of a preliminary cohort of participants scanned with photon-counting CT (PCCT) and energy-integrating detector (EID) CT on the same day, both modalities rated similarly for cortical (83 of 100 and 84 of 100, respectively) and trabecular discernibility (67 of 100 and 66 of 100, respectively).
- PCCT had radiation doses up to 83% lower than those in standard EID CT and showed no increase in perceived levels of image noise.
- There was no evidence of a difference in reader confidence for the detection of osteolytic lesions between PCCT and EID (78 of 100 and 76 of 100, respectively).

Keywords

CT, CT-Spectral, Skeletal-Axial, Spine, Hematologic Diseases, Whole-Body Imaging, Comparative Studies

Materials and Methods

Participants

In this Health Insurance Portability and Accountability Act–compliant, institutional review board–approved prospective study, all patients who underwent a clinical noncontrast CT multiple myeloma screening examination were invited to undergo a second scan with the PCCT system (NAEOTOM Alpha; Siemens Healthineers). All participants gave written informed consent, and no participants were excluded. Both scans were performed on the same day.

Multidetector CT Acquisition

Seven participants with known monoclonal gammopathy of undetermined significance were included who were referred to radiology for multiple myeloma screening on the basis of their clinical presentation between August and December 2021. All underwent noncontrast CT examination using a standard multiple myeloma screening protocol with a clinical EID CT scanner (Siemens SOMATOM Flash; Siemens Healthineers). A second scan was performed with PCCT using similar protocol parameters for the acquisition and reconstruction of images. CT examination z-axis coverage was from the level of the crown of the head through the feet, with scanning performed in the craniocaudal direction. CT images were reconstructed at 3-mm thickness with 1.5-mm increments. Automated tube current modulation was used for all examinations, and kilovoltage peak was set at 100 kVp/Sn140 for the EID scans and at 120 kVp for PCCT. Scan field of view was set to 50 cm, and displayed field of view was set for patient body size to include the entire abdomen.

Images were reconstructed with a Bv40f kernel for both systems, and measurements were performed on the mixed (120-kVp equivalent) images from the EID CT scans.

Quantitative Image Quality Analysis

Contrast-to-noise ratio (CNR) and signal-to-noise ratio (SNR) were calculated based on the largest possible regions of interest placed in the right paraspinal muscle (mean of 3 cm^2 in both modalities; range, 2–4 cm^2) and subcutaneous fat (mean of 1.8 cm^2 in both modalities; range, 1–2.8 cm^2) at the L1 level on three consecutive sections by one research fellow with 8 years of radiology experience (F.R.S.). Averages were calculated to account for inconsistencies in measurements. SNR was calculated as: $SNR_{skeletal\ muscle} = \text{Hounsfield unit (HU)}_{skeletal\ muscle}/SD_{skeletal\ muscle}$, and CNR was calculated as: $CNR_{skeletal\ muscle} = HU_{skeletal\ muscle} - HU_{fat})/SD_{fat}$, where $HU_{skeletal\ muscle}$ and HU_{fat} are the mean attenuation value of the skeletal muscle and fat, respectively, and $SD_{skeletal\ muscle}$ and SD_{fat} are the standard deviation of the skeletal muscle measurements and fat measurements, respectively (14,15).

Radiation dose measurements (volume CT dose index and dose-length product) were collected from both scanners.

Qualitative Image Quality Analysis

Five different locations within the scan were chosen to represent different levels of the spine and appendicular skeleton with varying likelihoods of multiple myeloma lesions: the dens axis, C5-C6 junction, T9, L5, and the level of hip articulation. There were a total of 35 images per method, yielding 70 total images (16,17) that were independently read by seven fellowship-trained diagnostic musculoskeletal radiologists (E.N.V., C.E.S., R.C., R.J.F., N.S., L.W., and E.M.) with 1–36 years of experience, providing 490 data points. A representative axial section with the same display settings (window width, 1500; window center, 450) from each CT method was shown to each reader in a randomized order to avoid introducing bias. Each reader rated the following characteristics: *(a)* the discernibility of the osseous cortex, *(b)* the discernibility of the osseous trabecules, *(c)* the perceived image noise level, and *(d)* reader confidence in making a diagnosis based on the image, shown on a continuous scale from 0 to 100. Each reader indicated whether a lytic osseous lesion was present or not. The presence or absence of an osteolytic lesion in the shown image was predetermined by one radiology fellow (F.R.S., 8 years of experience) on the basis of the clinical imaging report and image review in the picture archiving and communication system.

All readers received an interpretation handbook in the form of a Microsoft Word document with examples for each of the criteria at confidence ratings of 0, 50, and 100 for reference prior to making their decisions (Appendix E1 [supplement]); the examples were taken from a separate cohort to avoid image recall bias in readers.

Statistical Analysis

Descriptive statistics were used to characterize the participant sample. The quantitative image quality data were compared using paired *t* test with two tails. To compare reader scores,

Table 1: Participant Demographics

Parameter	Value
Age (y)	66 ± 9 (49–72)
Mean BMI (kg/m^2)	30.1 ± 5.2 (23.2–39.6)
No. of women	4
No. of men	3

Note.—Unless otherwise noted, data are means ± SDs, with ranges in parentheses. BMI = body mass index.

Table 2: Radiation Doses and Quantitative Imaging Parameters

Parameter	EID CT	PCCT
DLP (mGy·cm)	1654.1 ± 409.6 (1203–2307)	253.4 ± 89.6 (192–407)
$CTDI_{vol}$ (mGy)	11.37 ± 2.84 (7.9–15.6)	1.82 ± 0.63 (1.5–2.9)
SNR	2	4
CNR	13	13

Note.—Unless otherwise noted, data are means ± SDs, with ranges in parentheses. CNR = contrast-to-noise ratio, $CTDI_{vol}$ = volume CT dose index, DLP = dose-length product, EID = energy-integrating detector, PCCT = photon-counting CT, SNR = signal-to-noise ratio.

mixed effects linear modeling was used. To avoid biasing the results with clustering by readers or participants, scores were compared between imaging methods using mixed effects linear regression, with the imaging method treated as a fixed effect and with participant and reader as random effects. Interreader agreement was determined using intraclass correlation coefficient and Spearman rank correlation test. *P* value less than .05 was considered to indicate a significant difference. Statistical analysis was performed using RStudio Version 1.3.1056.

Results

Participant Characteristics

Seven participants (mean age, 66 years ± 9 [SD]; four women) were prospectively included; no participants were excluded. One participant had undergone prior surgery to treat a singular plasmocytoma lesion of the humerus (not present on study scans as an osteolytic lesion), one participant had several osteolytic lesions throughout the spine and pelvis, and one participant had a singular lesion in the L5 vertebrae. This led to the inclusion of four different sections with lesions in two participants (11% of the images shown to radiologists). Two of the lesions were subcentimeter size (0.9 × 0.6 cm and 0.5 × 0.7 cm), and two were greater than 1 cm in size (1.7 × 2 cm and 1.1 × 1 cm). The mean body mass index was 30.1 kg/m^2 ± 5.2, with a range of 23.2–39.6 kg/m^2 (Table 1).

Quantitative Analysis

Radiation doses and quantitative imaging parameters are shown in Table 2. CNR was similar between the modalities (EID vs PCCT: 13 vs 13, *P* = .96). While SNR differed between EID (2) and PCCT (4), this difference did not reach the level of statistical significance, with *P* = .09.

PCCT had lower radiation doses than conventional clinical scans when comparing volume CT dose index (EID: 11.37 ± 2.84 vs PCCT: 1.82 ± 0.63, *P* = .06) and dose-length product (EID: 1654.1 ± 409.6 vs PCCT: 253.4 ± 89.6, *P* = .05). Both measures represented an average of 83% radiation dose reduction.

Qualitative Analysis

A visual example of image quality in a participant with osteolytic lesions is shown in Figure 1, and an example of a participant without osteolytic lesions is shown in Figure 2.

Cortical delineation was ranked similarly for both PCCT and EID (mean score, 84 [95% CI: 82, 85] vs 83 [95% CI: 82, 84], respectively; *P* = .56) (Table 3). Trabecular delineation was also ranked similarly for both PCCT (mean score, 66 [95% CI: 63, 68]) and EID (mean score, 67 [95% CI: 65, 69]) (*P* = .11). Image noise was similar for the two acquisitions: PCCT mean score of 74 (95% CI: 72, 77) versus EID mean score of 75 (95% CI: 73, 77) (*P* = .26).

We found no evidence of a difference in diagnostic confidence. The PCCT images had a mean score of 76 (95% CI: 74, 79) versus EID with a mean score of 78 (95% CI: 76, 80) (*P* = .11).

A higher percentage of multiple myeloma lesions was detected using PCCT (79%, 22 of 28) compared with EID (64%, 18 of 28), although this did not represent a statistically significant difference (*P* = .18). There were more true-positive findings (19 vs 16) and fewer false-negative findings (nine vs 12) with PCCT than with EID (Fig 3). Most of the images represented the axial skeleton (55 of 70 images), but there was no evidence of a difference in the trends observed for the whole skeleton; PCCT images had more true-positive findings and fewer false-negative findings than did EID images (Figs E1, E2 [supplement]). Readers had the lowest percentage of detection for EID images of small (<1 cm) appendicular lesions at 43%, though large (>1 cm) axial lesions were detected at an equal rate of 86% in both modalities.

Interreader agreement was moderate, with intraclass correlation coefficients of 0.44 for cortical delineation, 0.55 for trabecular delineation, 0.53 for image noise, and 0.51 for diagnostic confidence. Readers were mostly consistent in their scores for PCCT and EID. For cortical delineation, all but one reader gave similar median scores, while the one outlier gave a higher median score to PCCT (Fig 4). For trabecular delineation and noise perception, all readers gave similar median scores to EID and PCCT (Fig 5, Fig E3 [supplement]). For diagnostic confidence, only one reader gave slightly lower scores to PCCT images (Fig 6).

Discussion

In participants with a clinical suspicion for multiple myeloma, this preliminary prospective head-to-head comparison of PCCT with conventional EID CT demonstrated similar image quality (cortical and trabecular delineation, image noise, and diagnostic confidence at *P* = .56, .11, .26, and .11, respec-

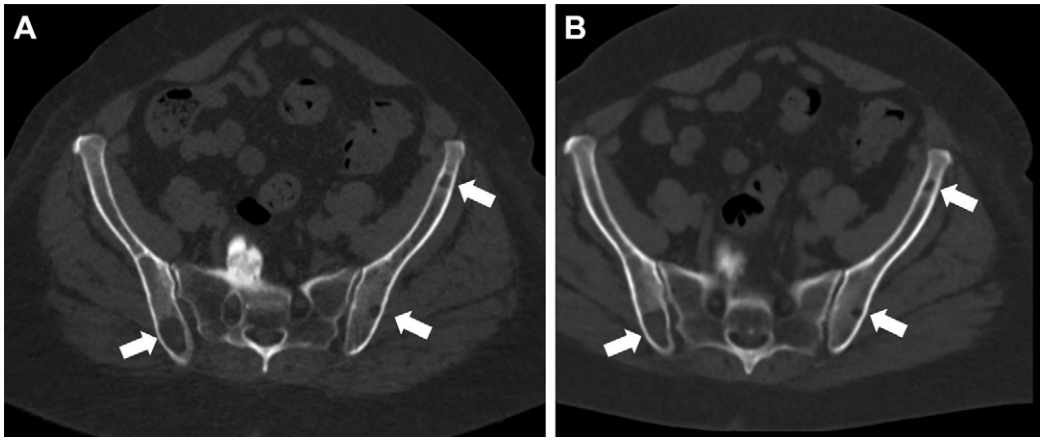

Figure 1: **(A)** Energy-integrating detector (EID) CT and **(B)** photon-counting CT (PCCT) images in a 71-year-old woman with a body mass index of 33 kg/m^2 and multiple lytic multiple myeloma lesions (white arrows). Dose-length product for this study was 1608 mGy·cm for EID and 257 mGy·cm for PCCT. Volume CT dose index was 11.3 mGy for EID and 1.8 mGy for PCCT.

Figure 2: **(A)** Energy-integrating detector (EID) CT and **(B)** photon-counting CT (PCCT) images in a 61-year-old man with a body mass index of 28 kg/m^2 and no multiple myeloma lesions. Dose-length product for this study was 1421 mGy·cm for EID and 213 mGy·cm for PCCT. Volume CT dose index was 9.04 mGy for EID and 1.47 mGy for PCCT.

Table 3: Mean Scores for Perceived Cortical and Trabecular Definition, Noise Levels, and Diagnostic Confidence

Parameter	EID Score	PCCT Score
Cortical delineation	83 ± 11	84 ± 12
Trabecular delineation	67 ± 18	66 ± 18
Image noise	75 ± 14	74 ± 17
Diagnostic confidence	78 ± 15	76 ± 17

Note.—Data are means ± SDs. No evidence of a difference was found between any of the energy-integrating detector (EID) CT and photon-counting CT (PCCT) scores.

tively) and osteolytic lesion detection (P = .18), with a significant radiation dose reduction of 83%.

Previous research on this topic consists of, to our knowledge, a solitary case report that suggests improved multiple myeloma lesion detection with PCCT (18). This study recommends using sharper reconstruction kernels (70 or higher) to improve lesion conspicuity, which may be a consideration for future research. We used the same kernel for PCCT as was used for clinical EID imaging (B40), as this was chosen by the department for the assessment of fat within lesions.

In addition to sharper kernel reconstructions, the inherent spectral capabilities of PCCT could be used to create color overlays based on tissue properties (eg, calcium as blue) to potentially aid lesion detection. While this article was under review, another study reported improved detection of multiple myeloma lesions with PCCT combined with deep learning reduction of noise relative to EID (19).

Our data are consistent with recent findings of PCCT demonstrating similar or superior image quality to standard CT imaging systems overall, with lower radiation dose (20). Our data also align with more-specific preclinical studies from Symons et al (21) who report improved image quality and lower radiation dose for calcium scoring performed with a PCCT prototype.

Though our cohort size was too small for detailed statistical analysis, we were able to see some trends in osteolytic lesion detection that align with what can be expected because of PCCT's inherently higher contrast resolution; the true-positive and false-negative detection rates were better for PCCT than for EID overall and for the axial and appendicular skeleton, respectively. In addition, EID had the lowest

All Readers	Actual Positive	Actual Negative
Answer Positive	35	72
Answer Negative	21	362

EID	Actual Positive	Actual Negative
Answer Positive	16	36
Answer Negative	12	174

PCCT	Actual Positive	Actual Negative
Answer Positive	19	36
Answer Negative	9	188

Figure 3: Confusion matrices for all images and readers combined and separated out according to imaging modality. There were more lesions detected and fewer missed lesions with PCCT than with EID CT. EID = energy-integrating detector, PCCT = photon-counting CT.

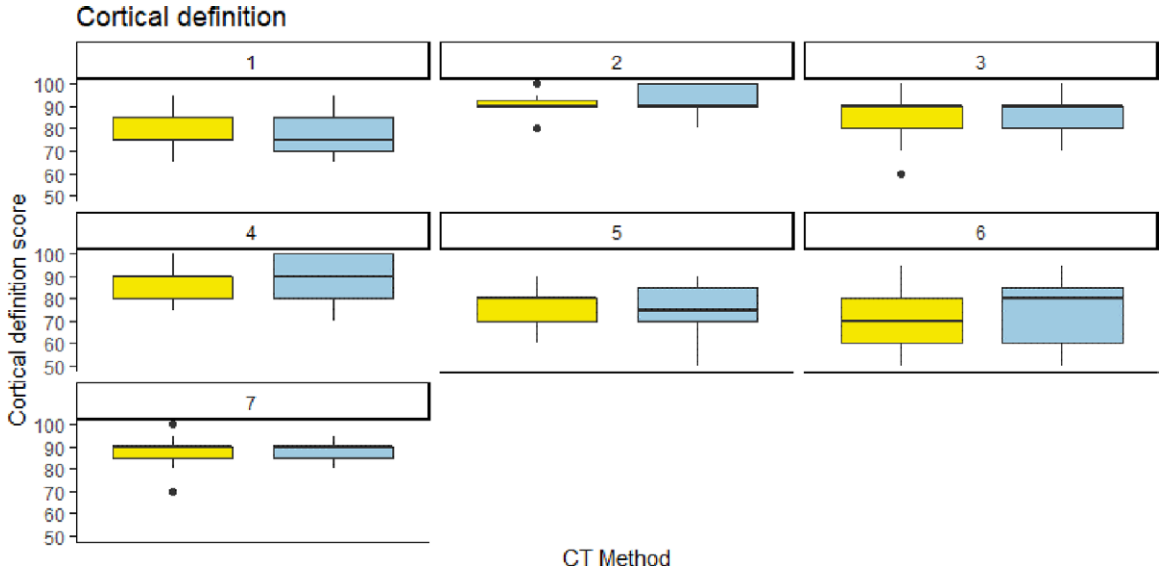

Figure 4: Individual reader scoring differences between energy-integrating detector CT (EID, yellow) and photon-counting CT (PCCT, blue) for cortical definition. Note that the median score was almost identical for both CT methods, save for one reader (reader 6) who rated the PCCT images slightly higher than the EID images.

detection rate for small (<1 cm) appendicular lesions, though the detection rate for larger (>1 cm) axial lesions was not affected by the imaging method.

The primary limitation of our study was the small sample size, which can lead to recall bias for readers, despite randomization of the order in which the images were shown, and low statistical power for some analyses. This can be attributed to the challenges of recruiting participants for a second whole-body CT scan and the fact that this was a single-center study.

Additionally, the scans in our study were standard radiation dose and therefore high relative to low-dose examinations for multiple myeloma screening as reported in the literature. With all other parameters adjusted as reported, PCCT might provide additional dose reduction potential (22). The intraclass correlation coefficient scores for reader agreement were only moderate, which was likely caused by the continuous scoring scale. For future evaluations, a five-point Likert scale might provide better agreement between readers. An additional potential limitation arises from the fact that PCCT is an emerging and developing technology compared to seasoned EID. Follow-up investigations using different reconstruction kernels may lead to continued improvement in PCCT diagnostic quality.

In conclusion, PCCT can provide similar quantitative image quality and equivalent qualitative reader scores for multiple myeloma screening as standard EID CT, at significantly reduced patient radiation doses. For patients who cannot undergo MRI for multiple myeloma screening, using PCCT for initial evaluation and follow-up could be beneficial.

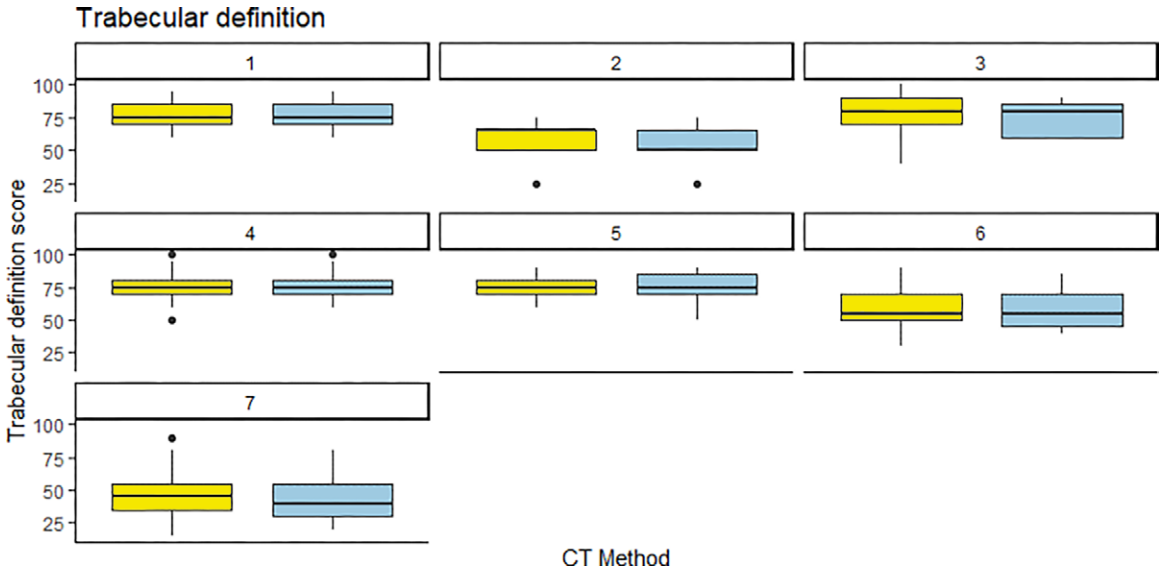

Figure 5: Individual reader scoring differences between energy-integrating detector CT (EID, yellow) and photon-counting CT (PCCT, blue) for trabecular definition. Note that the median score was almost identical for both CT methods, save for one reader (reader 2) who rated the PCCT images slightly lower than the EID images.

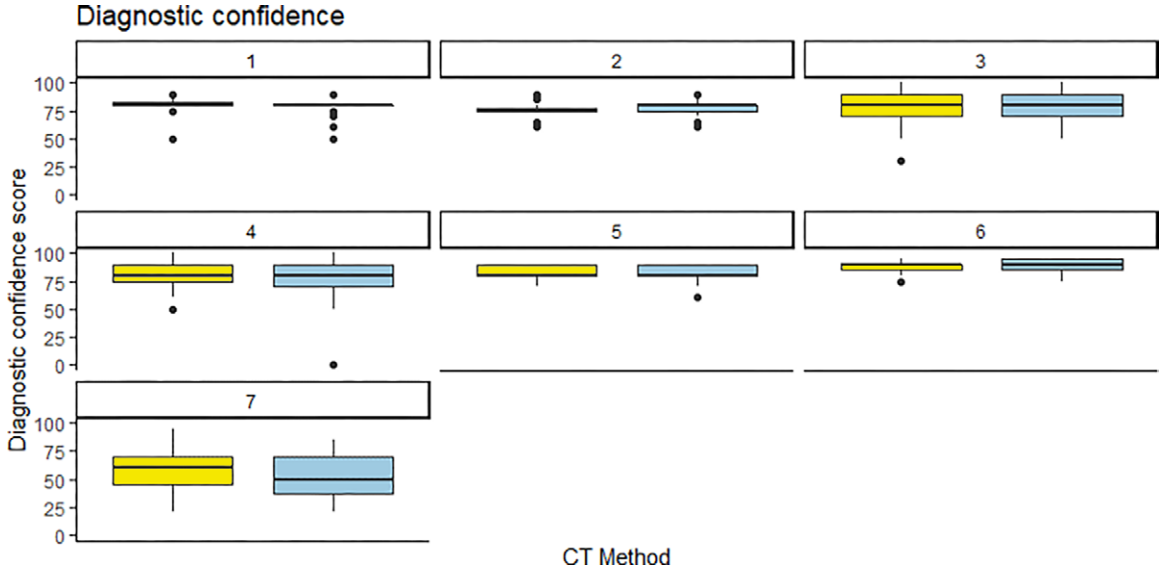

Figure 6: Individual reader scoring differences between energy-integrating detector CT (EID, yellow) and photon-counting CT (PCCT, blue) for diagnostic confidence. Note that the median score was almost identical for both CT methods, save for one reader (reader 6) who rated the PCCT images slightly higher than the EID images.

Acknowledgments: We would like to acknowledge the work of the CT team around Lior Molvin, RT (R) (CT), MBA, Dana Hawley, RT (R) (CT) (VI) ARRT, and Irving Arnold, RT (R) (CT) ARRT, for acquiring the image data, and our clinical research coordinator Elisabeth Luck, RT (R) (M) CCRC, for recruiting the participants for this study.

Author contributions: Guarantors of integrity of entire study, **F.R.S., R.J.F., N.S.**; study concepts/study design or data acquisition or data analysis/interpretation, all authors; manuscript drafting or manuscript revision for important intellectual content, all authors; approval of final version of submitted manuscript, all authors; agrees to ensure any questions related to the work are appropriately resolved, all authors; literature research, **F.R.S., R.C., E.S., E.M.;** clinical studies, **F.R.S., E.N.V., C.E.S., R.C., E.S., R.J.F., N.S., E.M.;** statistical analysis, **F.R.S.**; and manuscript editing, **F.R.S., E.N.V., R.C., E.S., R.J.F., N.S., L.W., E.M.**

Disclosures of conflicts of interest: F.R.S. Payment or honoraria from Siemens Healthineers for educational luncheon presentation at Society of Thoracic Radiology (STR) March 2022, Las Vegas; support from Siemens Healthineers for travel to STR 2022; participation on a photon-counting CT advisory board for Siemens Healthineers (no financial compensation). **E.N.V.** No relevant relationships. **C.E.S.** Royalties or licenses from Now UptoDate for the "Imaging of osteomyelitis" section. **R.C.** No relevant relationships. **E.S.** Research funding for this work from Siemens Healthineers; grants or contracts from GE and Siemens; royalties or licenses from GE, SunNuclear, XCAT, and Metis Health Analytics; consulting fees from Nanox; payment or honoraria for lectures, presentations, speakers bureaus, manuscript writing, or education events from Cambridge University Press and Wiley and Sons; payment from Rubin Anders for expert testimony; participation on a DataSafety Monitoring Board or Advisory Board for Imalogix, Metis Health Analytics, GE, and Siemens; leadership or fiduciary role in the American Association of Physicists in Medicine (AAPM). **R.J.F.** No relevant relationships. **N.S.** No relevant relationships. **L.W.** No relevant relationships. **E.M.** No relevant relationships.

References

1. Terpos E, Kleber M, Engelhardt M, et al; European Myeloma Network. European Myeloma Network guidelines for the management of multiple myeloma-related complications. Haematologica 2015;100(10):1254–1266.
2. Moreau P, San Miguel J, Sonneveld P, et al; ESMO Guidelines Committee. Multiple myeloma: ESMO Clinical Practice Guidelines for diagnosis, treatment and follow-up. Ann Oncol 2017;28(suppl_4):iv52–iv61.
3. Ormond Filho AG, Carneiro BC, Pastore D, et al. Whole-body imaging of multiple myeloma: diagnostic criteria. RadioGraphics 2019;39(4):1077–1097.
4. Cowan AJ, Green DJ, Kwok M, et al. Diagnosis and management of multiple myeloma: a review. JAMA 2022;327(5):464–477.
5. van de Donk NWCJ, Pawlyn C, Yong KL. Multiple myeloma. Lancet 2021;397(10272):410–427.
6. Rajkumar SV. The screening imperative for multiple myeloma. Nature 2020;587(7835):S63.
7. Di Giuliano F, Picchi E, Muto M, et al. Radiological imaging in multiple myeloma: review of the state-of-the-art. Neuroradiology 2020;62(8):905–923.
8. Albert JM. Radiation risk from CT: implications for cancer screening. AJR Am J Roentgenol 2013;201(1):W81–W87.
9. Yamashita K, Higashino K, Hayashi H, et al. Direct measurement of radiation exposure dose to individual organs during diagnostic computed tomography examination. Sci Rep 2021;11(1):5435. [Published correction appears in Sci Rep 2022;12(1):5035.]
10. McCollough CH, Leng S, Yu L, Fletcher JG. Dual- and multi-energy ct: principles, technical approaches, and clinical applications. Radiology 2015;276(3):637–653.
11. Flohr T, Petersilka M, Henning A, Ulzheimer S, Ferda J, Schmidt B. Photon-counting CT review. Phys Med 2020;79:126–136.
12. Leng S, Bruesewitz M, Tao S, et al. Photon-counting Detector CT: System design and clinical applications of an emerging technology. RadioGraphics 2019;39(3):729–743.
13. Willemink MJ, Persson M, Pourmorteza A, Pelc NJ, Fleischmann D. Photon-counting CT: technical principles and clinical prospects. Radiology 2018;289(2):293–312.
14. Leng S, Yu L, Fletcher JG, McCollough CH. Maximizing iodine contrast-to-noise ratios in abdominal CT imaging through use of energy domain noise reduction and virtual monoenergetic dual-energy CT. Radiology 2015;276(2):562–570.
15. Wellenberg RH, Boomsma MF, van Osch JA, et al. Quantifying metal artefact reduction using virtual monochromatic dual-layer detector spectral CT imaging in unilateral and bilateral total hip prostheses. Eur J Radiol 2017;88:61–70.
16. Bier G, Kloth C, Schabel C, Bongers M, Nikolaou K, Horger M. Vertebral lesion distribution in multiple myeloma--assessed by reduced-dose whole-body MDCT. Skeletal Radiol 2016;45(1):127–133.
17. Larbi A, Omoumi P, Pasoglou V, et al. Comparison of bone lesion distribution between prostate cancer and multiple myeloma with whole-body MRI. Diagn Interv Imaging 2019;100(5):295–302.
18. Wehrse E, Klein L, Kachelrieß M, et al. First experience in man with an ultra-high resolution whole-body photon-counting CT for oncologic imaging. Vienna, Austria: European Congress of Radiology, 2020.
19. Baffour FI, Huber NR, Ferrero A, Rajendran K, et al. Photon-counting detector CT with deep learning noise reduction to detect multiple myeloma. Radiology doi:10.1148/radiol.220311. Published online September 6, 2022.
20. Rajendran K, Petersilka M, Henning A, et al. First clinical photon-counting detector CT system: technical evaluation. Radiology 2022;303(1):130–138.
21. Symons R, Sandfort V, Mallek M, Ulzheimer S, Pourmorteza A. Coronary artery calcium scoring with photon-counting CT: first in vivo human experience. Int J Cardiovasc Imaging 2019;35(4):733–739.
22. Baldi D, Tramontano L, Alfano V, Punzo B, Cavaliere C, Salvatore M. Whole body low dose computed tomography using third-generation dual-source multidetector with spectral shaping: protocol optimization and literature review. Dose Response 2020;18(4):1559325820973131.